Int. J. Open Problems Compt. Math., Vol. 3, No. 3, September 2010
ISSN 1998-6262; Copyright © ICSRS Publication, 2010
www.i-csrs.org

A Refined Solution to The Problem of Torsion of A Viscoelastic Anisotropic Reinforced Layer

M.N.M. Allam[1], N.A. El-Bedwehy[2], and R. Tantawy[2]

[1] Mathematics Department, Faculty of Science, Mansoura University, Mansoura 35516, Egypt
e mail: mallam@mans.edu.eg
[2]Mathematics Department, Faculty of Science, Mansoura University, Damietta, Egypt
e mail: rania_eltantwy@yahoo.com

Abstract

This paper proposes a novel innovative scheme for formal solution of the stresses and displacement, occurring in an infinite anisotropic layer, when it is twisted by means of a rigid cylindrical shaft attached to it. In this research, the problem is modified by considering the layer is made of a viscoelastic material reinforced by elastic fibers, and by using the method of effective moduli, the non-homogeneous isotropic layer is transferred to homogeneous layer (structurally anisotropic). The motivation behind such idea is to find the distributions of stresses and displacement in this model. The behavior of the layer is governed by the equilibrium equations, which solved by means of Hankel transforms. The dynamic mixed boundary value problem can lead to dual integral equations as a first step. The solution of purely elastic layer is analytically obtained, and then the problem of structurally anisotropic reinforced viscoelastic layer is solved using the correspondence principle and Illyushin's approximation method. A numerical example is given and the fields of stress and displacement are illustrated.

Keywords: *Torsion, Shafts, Viscoelasticity, Anisotropic material, Elastic layer, Dual integral equation.*

1 Introduction

Torsion of anisotropic viscoelastic reinforced layer represents both crucial and challenge process in number of composite materials within distinct real-world engineering industry for example, dams, machine foundations and similar large structures, and have gained considerable attention in many engineering applications. Composite materials are microscopically inhomogeneous, in which the mechanical properties vary from one point to another or one surface to another. The general stability of drive shafts under torsion has been studied by many researchers. The torsion problem of an anisotropic layer with fixed base on a rigid foundation when it is twisted by means of turning an attached rigid cylindrical shaft studied by Tang, 1979 [15], the solution is given at some levels (the base and upper surface).

Allam et al, 1982 [9], studied torsion of a composite viscoelastic prismatic bar of rectangular cross-section, they used the generalization of Illyushin's approximation method to determine the stresses in the quasi-static problem of torsion of a composite viscoelastic prismatic bar of rectangular cross-section. Chen et al, 1998[8], using a finite element method to study the stability of composite shafts under rotation and axial compression load, they predicated the critical axial load of a thin-wall composite shaft under rotation. Nayfeh et al, 2003 [17], studied a model for torsional vibration of slender thin-walled tubes with constrained layer dampers, they developed a suitable model for prediction of the complex stiffness per unit length in closed thin walled tubes, whose walls consist of laminated elastic and viscoelastic layers, and formulate a boundary-value problem for the warping deformations arising under Saint-Venant torsion.

Shokrieh et al, 2004 [14], studied the torsional stability of composite drive shaft torsion, composite materials are considered as the suitable choice for manufacturing long drive shafts.

Tarn et al, 2007 [6], studied the torsion of elastic circular bars of radial in-homogeneous, cylindrically orthotropic materials, with emphasis on the end effects. They examined the conjecture of Saint-Venant's torsion, and considered torsion of circular bars, with one end fixed and the other end free, on which tractions that results in a pure torque are prescribed arbitrarily over the free end surface.

Methods of solving quasi-static viscoelastic problems in a reinforced composite material have been developed by Allam et al, 1976 [12]. Allam et al, 2003 [11], they used the small parameter method as well as the method of effective module for the bending response of a reinforced viscoelastic arched bridge model. Allam et al, 2005 [10], have studied the rotating of viscoelastic solid and annular disks of exponentially varying thickness by analytical means. The material is assumed to be fiber reinforced viscoelastic composite. The effects due to many parameters on the stresses and displacements of rotating solid and annular disks are investigated. Allam, et al, 2008 [13], considered a circular elastic disk (conductor) of variable thickness under the influence of a steady coaxial current and bearing a coaxial

viscoelastic coating (insulator), in both conductor and insulator there exist a heat source generation. As a first step, the solution of purely elastic conductor and insulator is obtained. Then the problem of model with viscoelastic coating is solved using the correspondence principle and Illyushin's approximation method. Aseeri, 2008 [16], present mapping function deals with famous shapes of tunnels, then it is useful to use it in studying stresses and strains around tunnels. Dewa, 1989 [4], generates numerical solution for three layer elastic-viscoelastic beams made up of solid rectangular laminate. Other researches have studied bending and torsion of laminated rectangular beams composed anisotropic laminates such as Napolitano et al, 1998 [7], and Nouri-Baranger et al, 1999 [19].

In this paper we consider the problem of a structurally anisotropic viscoelastic layer with fixed base when it is twisted by means of an attached rigid cylindrical shaft. The solution was modified by adding some terms which are canceled in the Tang's solution 1979 [15], and then we suppose that the layer is made of composite viscoelastic material. The main objective is to find the distributions of stresses and displacement in this model.

2 Formulation of the Problem

Consider the anisotropic layer whose material has three mutually perpendicular directions of elasticity symmetry parallel to the axis of coordinates. For such material the equations of the generalized Hooke's law is written in the following way (Lekhnitskii, 1987 [18]):

$$\begin{aligned}
\varepsilon_r &= \frac{\partial u_r}{\partial r} = s_{11}\sigma_r + s_{12}\sigma_\theta + s_{13}\sigma_z & \varepsilon_{\theta z} &= \frac{\partial u_\theta}{\partial z} + \frac{1}{r}\frac{\partial u_z}{\partial \theta} = s_{44}\sigma_{\theta z} \\
\varepsilon_\theta &= \frac{1}{r}\frac{\partial u_\theta}{\partial \theta} + \frac{u_r}{r} = s_{12}\sigma_r + s_{22}\sigma_\theta + s_{23}\sigma_z & \varepsilon_{zr} &= \frac{\partial u_z}{\partial r} + \frac{\partial u_r}{\partial z} = s_{55}\sigma_{zr} \\
\varepsilon_z &= \frac{\partial u_z}{\partial z} = s_{13}\sigma_r + s_{23}\sigma_\theta + s_{33}\sigma_z & \varepsilon_{r\theta} &= \frac{1}{r}\frac{\partial u_r}{\partial \theta} + \frac{\partial u_\theta}{\partial r} - \frac{u_\theta}{r} = s_{66}\sigma_{r\theta}
\end{aligned} \quad , \quad (1)$$

where s_{ij} are elastic constant's of the layer, u_r, u_θ and u_z are the displacements with references to (r,θ,z) coordinates respectively, $\varepsilon_r, \varepsilon_\theta, \varepsilon_z, \varepsilon_{\theta z}, \varepsilon_{r\theta}$ and ε_{rz} are the strain components, $\sigma_r, \sigma_\theta, \sigma_z, \sigma_{\theta z}, \sigma_{r\theta}$ and σ_{rz} are the stress components in cylindrical coordinate.

Let us take (see Fig.1) the axis of the cylindrical shaft as the z -axis of a cylindrical coordinate system (r,θ,z) the origin being at the centre of the cross section of the shaft which attached to the layer, a is the radius of the cylindrical shaft and h is the thickness of the layer. The polar r -axis is directed arbitrarily. It is assumed that

one of the boundary surface $(z = h)$ is fixed and the other surfaces of the layer $(z = 0)$ is subjected to a torsion Ω over the area $0 \le r \le a$ and let $a < h$.

It is assumed that the cross sections of the layer are not rotated and the displacements in the radial and axial directions are absent, that is:

$$u_r = 0 \quad , \quad u_\theta = u_\theta(r,z) \quad , \quad u_z = 0,$$

Then, from equation (1) all the components of stress vanish identically except $\sigma_{\theta z}$ and $\sigma_{r\theta}$ which are given by the relations

$$\sigma_{\theta z} = \frac{1}{s_{44}} \frac{\partial u_\theta}{\partial z} \quad \& \quad \sigma_{r\theta} = \frac{1}{s_{66}} \left(\frac{\partial u_\theta}{\partial r} - \frac{u_\theta}{r} \right), \tag{2}$$

the remaining two components of stress $\sigma_{\theta z}$ and $\sigma_{r\theta}$ depend only on r and z , and by using the equations of equilibrium (Lekhnitskii, 1987 [18]):

$$\left.\begin{aligned} &\frac{\partial \sigma_r}{\partial r} + \frac{1}{r}\frac{\partial \sigma_{r\theta}}{\partial \theta} + \frac{\partial \sigma_{zr}}{\partial z} + \frac{\sigma_r - \sigma_\theta}{r} = 0 \\ &\frac{\partial \sigma_{r\theta}}{\partial r} + \frac{1}{r}\frac{\partial \sigma_{\theta\theta}}{\partial \theta} + \frac{\partial \sigma_{\theta z}}{\partial z} + 2\frac{\sigma_{r\theta}}{r} = 0 \\ &\frac{\partial \sigma_{zr}}{\partial r} + \frac{1}{r}\frac{\partial \sigma_{\theta z}}{\partial \theta} + \frac{\partial \sigma_z}{\partial z} + \frac{\sigma_{zr}}{r} = 0 \end{aligned}\right\}.$$

The first and third equations are directly vanished, and the second equation becomes:

$$\frac{\partial^2 u_\theta}{\partial r^2} + \frac{1}{r}\frac{\partial u_\theta}{\partial r} - \frac{u_\theta}{r^2} + k\,\frac{\partial^2 u_\theta}{\partial z^2} = 0, \qquad k = \frac{s_{66}}{s_{44}} \tag{3}$$

the mixed boundary conditions are assumed to be:

$$u_\theta\big|_{r=0} = 0 \tag{4.a}$$

$$u_\theta\big|_{z=h} = 0 \tag{4.b}$$

$$u_\theta\big|_{\substack{z=0 \\ r<a}} = \Omega r \tag{4.c}$$

$$\frac{\partial u_\theta}{\partial z}\Big|_{\substack{z=0 \\ r>a}} = s_{44}\sigma_{\theta z}\Big|_{\substack{z=0 \\ r>a}} = 0 \tag{4.d}$$

where Ω is the angular displacement of the shaft.

The solution of the equation (3) has the form:

$$u_\theta(r,z) = \int_0^\infty \left(B_1 \cosh\left(\frac{p\,z}{\sqrt{k}}\right) + B_2 \sinh\left(\frac{p\,z}{\sqrt{k}}\right) \right) J_1(pr)\,dp,$$

where B_1, B_2 is a constant and J_1 is the first Bessel function. From boundary conditions Equation (4.a) and equation (4.b) and assuming that at infinity $(r \to \infty)$ the displacement u_θ must remain finite, then by the use of Hankel transform the general solution of the differential equation takes the form:

$$u_\theta(r,z) = \int_0^\infty A(p) \frac{\sinh\left[\frac{p}{\sqrt{k}}(h-z)\right]}{\sinh\left(\frac{p\,h}{\sqrt{k}}\right)} J_1(p\,r)\,d\,p \tag{5}$$

where, $A(p)$ is the unknown function determine from boundary conditions.
It follows from equation (2) that the non-vanishing components of stress are:

$$\left.\begin{aligned} \sigma_{\theta z} &= \frac{1}{s_{44}}\frac{\partial u_\theta}{\partial z} = -\frac{1}{s_{44}\sqrt{k}} \int_0^\infty p\,A(p) \frac{\cosh\left[\frac{p}{\sqrt{k}}(h-z)\right]}{\sinh\left(\frac{p\,h}{\sqrt{k}}\right)} J_1(p\,r)\,d\,p \\ \sigma_{r\theta} &= \frac{1}{s_{66}}\left(\frac{\partial u_\theta}{\partial r} - \frac{u_\theta}{r}\right) = -\frac{1}{s_{66}} \int_0^\infty p\,A(p) \frac{\sinh\left[\frac{p}{\sqrt{k}}(h-z)\right]}{\sinh\left(\frac{p\,h}{\sqrt{k}}\right)} J_2(p\,r)\,d\,p \end{aligned}\right\}, \tag{6}$$

where J_2 is the second order Bessel function.

Using the boundary conditions on $z = 0$ in equations (4.c), (4.d) we get the equations:

$$\left.\begin{aligned} &\int_0^\infty A(p) J_1(pr)\,dp = \Omega r && 0 \le r \le a \\ &\int_0^\infty p\,A(p) \coth\left(\frac{ph}{\sqrt{k}}\right) J_1(pr)\,dp = 0 && a < r < \infty \end{aligned}\right\} \tag{7}$$

Putting $p\,A(p)\coth(pb) = f(p)$, where $b = \frac{h}{\sqrt{k}}$, then the equations (7) become the dual integral equations:

$$\left.\begin{aligned} &\int_0^\infty p^{-1} \tanh(pb) f(p) J_1(pr)\,dp = \Omega\, r && 0 \le r \le a \\ &\int_0^\infty f(p) J_1(pr)\,dp = 0 && a < r < \infty \end{aligned}\right\}. \tag{8}$$

Using Tranter's method (Tranter, 1962 [1]), we have

$$f\ (p)=\frac{\Omega(2p)^{1-\alpha}}{\Gamma(1+\alpha)}\sum_{n=0}^{\infty}(\delta_{n0}-c_n+c_n'-c_n''+\cdots)J_{2n+\alpha+1}(a\ p) \tag{9}$$

where α is a real and positive number. Γ is the gamma function, and δ_{n0} is the kronecker delta symbol and

$$c_n=L_{0,n}\quad,\quad c_n'=\sum_{m=0}^{\infty}L_{m,n}\,c_m\quad,\quad c_n''=\sum_{m=0}^{\infty}L_{m,n}\,c_m'\quad,... \tag{10}$$

for $b>1$, we may choose $\alpha=\frac{1}{2}$ (Tranter, 1962 [1]), then:

$$L_{m,n}=(4n+3)\int_0^{\infty}p^{-1}\left(\tanh(p\,b)-1\right)J_{2m+\frac{3}{2}}(a\,p)J_{2n+\frac{3}{2}}(a\,p)d\ p \tag{11}$$

writing the hyperbolic function as a series of exponentials, the equation (11) becomes:

$$\frac{1}{(8n+6)}L_{m,n}=\sum_{q=1}^{\infty}(-1)^q\int_0^{\infty}p^{-1}e^{(-2q\,b\,p)}J_{2m+\frac{3}{2}}(a\,p)J_{2n+\frac{3}{2}}(a\,p)d\ p \tag{12}$$

The right hand side of this equation can be expressed as a power series in $\left(2qh/\sqrt{k}\right)^{-1}$ by using the formula given by Whittaker and Watson, 1965 [2]. Doing this and interchange the order of summation yield,

$$\int_0^{\infty}e^{-2qbp}p^{-1}J_{2m+\frac{3}{2}}(qp)J_{2n+\frac{3}{2}}(qp)dp=$$

$$\sum_{t=0}^{\infty}(-1)^t\frac{\Gamma(2n+2m+2t+3)\Gamma(2m+2n+2t+4)}{t!\Gamma\left(2m+t+\frac{5}{2}\right)\Gamma\left(2n+t+\frac{5}{2}\right)\Gamma(2m+2n+t+4)}\left(\frac{\beta}{4}\right)^{2m+2n+2t+3}q^{-2m-2n-2t-3}$$

where $\beta=\frac{a}{b}=\frac{a}{h}\sqrt{k}$, the equation (12) may written as:

$$\frac{1}{(8n+6)}L_{m,n}=\sum_{t=0}^{\infty}(-1)^{t+1}D_1\left(\frac{\beta}{4}\right)^{2m+2n+2t+3}\left(1-2^{1-(2m+2n+2t+3)}\right)\zeta(2m+2n+2t+3) \tag{13}$$

where $D_1=\dfrac{\Gamma(2n+2m+2t+3)\Gamma(2m+2n+2t+4)}{t!\Gamma\left(2m+t+\frac{5}{2}\right)\Gamma\left(2n+t+\frac{5}{2}\right)\Gamma(2m+2n+t+4)}$

and $\zeta(t)$ is Rieman's zeta function. Then $L_{m,n}$ may be determine to any degree of approximation according to the power of $\beta(\beta<<1)$. For the seventh power of β we have:

$$\left.\begin{aligned}
L_{0,0} &= \tfrac{-1}{4\pi}\left(\beta^3\zeta(3)-\tfrac{3}{4}\beta^5\zeta(5)+\tfrac{81}{160}\beta^7\zeta(7)\right)\\
L_{0,1} &= \tfrac{-1}{4\pi}\left(\tfrac{1}{4}\beta^5\zeta(5)-\tfrac{49}{160}\beta^7\zeta(7)\right)\\
L_{1,0} &= \tfrac{-3}{4\pi}\left(\tfrac{1}{8}\beta^5\zeta(5)-\tfrac{61}{4\pi}\beta^7\zeta(7)\right)\\
L_{1,1} &= \tfrac{-9}{640\pi}\beta^7\zeta(7)\\
L_{0,2} &= \tfrac{-1}{128\pi}\beta^7\zeta(7)\\
L_{2,0} &= \tfrac{-3}{1408\pi}\beta^7\zeta(7)
\end{aligned}\right\} \qquad (14)$$

All the other $L_{m,n}$ are negligible since the power of β greater than 7. Substitute of equation (14) in equation (10), we find the values of c_i :

$$\begin{aligned}
c_0 &= \tfrac{-1}{4\pi}\left[\beta^3\zeta(3)-\tfrac{3}{4}\beta^5\zeta(5)+\tfrac{81}{160}\beta^7\zeta(7)\right]\\
c_1 &= \tfrac{-1}{16\pi}\left[\beta^5\zeta(5)-\tfrac{49}{40}\beta^7\zeta(7)\right]\\
c_2 &= \tfrac{-1}{128\pi}\beta^7\zeta(7)\\
c_0' &= \tfrac{1}{18\pi}\beta^6\zeta(3)\zeta(3)\\
c_1' &= c_2' = c_0'' = c_1'' = c_2'' = 0
\end{aligned} \qquad (15)$$

Using the above mentioned values, equation (10) yields:

$$f(p) = \Omega(2p)^{\frac{1}{2}}\sum_{n=0}^{\infty}\frac{1}{\Gamma\left(\frac{3}{2}\right)}\left[\delta_{n0}-c_n+c_n'-c_n''+\cdots\right]J_{2n+\frac{3}{2}}(ap)$$

$$= \Omega\sqrt{\frac{8p}{\pi}}\left[\left[1-c_0+c_0'-c_0''\right]J_{\frac{3}{2}}(ap)+\left[-c_1+c_1'-c_1''\right]J_{\frac{7}{2}}(ap)+\left[-c_2+c_2'-c_2''\right]J_{\frac{11}{2}}(ap)\right]$$

So by using equation (15)

$$f(p) = \Omega\sqrt{\frac{8p}{\pi}}\left[H_0\,J_{\frac{3}{2}}(ap)+H_1\,J_{\frac{7}{2}}(ap)+H_2\,J_{\frac{11}{2}}(ap)\right] \qquad (16)$$

Then the function $A(p)$ may found as:

$$A(p) = \Omega\sqrt{\frac{8}{\pi p}}\tanh(pb)\left[H_0\,J_{\frac{3}{2}}(ap)+H_1\,J_{\frac{7}{2}}(ap)+H_2\,J_{\frac{11}{2}}(ap)\right] \qquad (17)$$

where

$$H_0 = 1 + \frac{1}{4\pi}\left(\beta^3\zeta(3) - \frac{3}{4}\beta^5\zeta(5) + \frac{81}{640}\beta^7\zeta(7)\right) + \frac{1}{16\pi^2}\beta^6\zeta(3)\zeta(3),$$

$$H_1 = \frac{1}{16\pi}\left(\beta^5\zeta(5) - \frac{49}{40}\beta^7\zeta(7)\right), \quad H_2 = \frac{-1}{128\pi}\beta^7\zeta(7).$$

The displacement and stresses can then be found from equation (6).

When h is sufficiently large (i.e. for an elastic half-space), using the asymptotic expansions given by Whittaker and Watson,1965 [2], and Watson,1966 [3] follows:

$$f(p) = 2\Omega\sqrt{\tfrac{2P}{\pi}}J_{\frac{3}{2}}(ap)$$

$$= \tfrac{4\Omega}{\pi}\left(\tfrac{\sin(a\,p)}{\sqrt[3]{a\,p}} - \cos(ap)\right)$$

this is the expression for half-space given by (Sneddon, 1966 [5]) in the isotropic case.

3.1 The elastic solution

The numerical solutions of stresses and displacement are directly evaluated from equation (5) and equation (6) with the result of $f(p)$ and $A(p)$ may be written as:

$$\left.\begin{aligned}
u_\theta(r,z) &= \Omega\sqrt{\tfrac{8}{\pi}}\int_0^\infty p^{-\frac{1}{2}}\tanh(pb)\frac{\sinh\left[\frac{p}{\sqrt{k}}(h-z)\right]}{\sinh(pb)}D_2\,J_1(p\,r)dp \\
\sigma_{\theta z}(r,z) &= \tfrac{-\Omega}{s_{44}}\sqrt{\tfrac{8}{\pi k}}\int_0^\infty p^{\frac{1}{2}}\tanh(pb)\frac{\cosh\left[\frac{p}{\sqrt{k}}(h-z)\right]}{\sinh(pb)}D_2J_1(p\,r)dp \\
\sigma_{r\theta}(r,z) &= \tfrac{-\Omega}{s_{66}}\sqrt{\tfrac{8}{\pi}}\int_0^\infty p^{\frac{1}{2}}\tanh(pb)\frac{\sinh\left[\frac{p}{\sqrt{k}}(h-z)\right]}{\sinh(pb)}D_2\,J_2(p\,r)dp
\end{aligned}\right\} \qquad (18)$$

where $D_2 = H_0\,J_{\frac{3}{2}}(a\,p) + H_1\,J_{\frac{7}{2}}(a\,p) + H_2\,J_{\frac{11}{2}}(a\,p)$

The final forms for stresses and displacement are directly evaluated, using the appendix equations is as follows:

$$u_\theta(r,z) = \frac{2\Omega}{\sqrt{a}}\begin{cases}\frac{2}{3\pi}B_1(1) & r \le a\\ \frac{r}{\sqrt{\pi}}B_2(1) & r \ge a\end{cases}$$

$$\sigma_{\theta z}(r,z) = \frac{-4\Omega}{s_{44}\sqrt{a\,k}}\begin{cases}\frac{1}{3\pi}B_1(2) & r \le a\\ \frac{r}{\sqrt{\pi}}B_2(2) & r \ge a\end{cases}$$

$$\sigma_{r\theta}(r,z) = \frac{-4\Omega}{s_{66}\sqrt{a}}\begin{cases}\frac{4}{3\pi}B_1(3) & r \le a\\ \frac{r^2}{\sqrt{\pi}}B_2(3) & r \ge a\end{cases}$$

The expressions for $B_1(k), B_2(k),\ k = 1,2,3$ are given in the appendix.

3.2 Viscoelastic Composite layer:

Now, consider the solution for the case of a layer made of viscoelastic isotropic material (filler) reinforced by elastic isotropic fibers, this material is considered as structurally anisotropic material, where

$$S_{66} = \frac{1}{G_{12}}, \quad S_{44} = \frac{1}{G_{23}} \tag{19}$$

Let the viscoelastic filler be characterized by Young's modulus E_1, shear modulus G_1, and Poisson ratio υ_1, or by the bulk modulus K and dimensionless kernel of relaxation $\omega(t)$, while the elastic reinforcement be characterized by E, υ, G; where

$$\begin{aligned} E &= 2G(1+\upsilon)\\ \upsilon_1 &= \frac{1-\omega}{2+\omega}, \quad E_1 = \frac{9K\omega}{2+\omega}, \quad G_1 = \frac{3}{2}K\omega \end{aligned} \tag{20}$$

Let $K = \xi E$, and γ is the ratio volume fraction of the reinforcement to the volume the whole material. Then for the composite viscoelastic layer we get,

$$G_{23} = \gamma G + (1-\gamma)G_1$$

$$= E\left[\frac{\gamma + 3(1-\gamma)\xi\omega(1+\upsilon)}{2(1+\upsilon)}\right]$$

$$\frac{1}{G_{12}} = \frac{\gamma}{G} + \frac{(1-\gamma)}{G_1}$$

$$G_{12} = E\,\frac{3\omega\xi}{6\gamma\omega\xi(1+\upsilon)+2(1-\gamma)}$$

so from these relations we can write the ratio $k = \frac{s_{66}}{s_{44}}$ in the form

$$k=\gamma^2\left[\frac{3\gamma^2\omega\xi(1+\upsilon_1)+\gamma(1-\gamma)+9\gamma\omega^2\xi^2(1-\gamma)(1+\upsilon_1)^2+3\omega\xi(1+\upsilon_1)(1-\gamma)^2}{3\gamma^2\omega\xi(1+\upsilon_1)}\right] \tag{21}$$

Suppose that $\bar{\sigma}_{r\theta}=\frac{\sigma_{r\theta}}{E_1}, \bar{\sigma}_{\theta z}=\frac{\sigma_{\theta z}}{E_1}$ are the dimensionless stresses. The equations (6) become after removing the bar symbol

$$\left.\begin{aligned}
u_\theta &= \int_0^\infty A(p)\frac{\sinh\left[\frac{p}{\sqrt{k}}(h-z)\right]}{\sinh\left(\frac{p\,h}{\sqrt{k}}\right)}J_1(p\,r)d\,p\\
\sigma_{r\theta} &= -\left[\frac{3\omega\xi}{6\gamma\omega\xi(1+\upsilon_1)+2(1-\gamma)}\right]\int_0^\infty p\,A(p)\frac{\sinh\left[\frac{p}{\sqrt{k}}(h-z)\right]}{\sinh\left(\frac{p\,h}{\sqrt{k}}\right)}J_2(p\,r)d\,p\\
\sigma_{\theta z} &= -\sqrt{\frac{3\omega\xi\gamma+9(1-\gamma)\omega^2\xi^2(1+\upsilon_1)}{12\gamma\omega\xi(1+\upsilon_1)^2+4(1+\upsilon_1)(1-\gamma)}}\int_0^\infty p\,A(p)\frac{\cosh\left[\frac{p}{\sqrt{k}}(h-z)\right]}{\sinh\left(\frac{p\,h}{\sqrt{k}}\right)}J_1(p\,r)d\,p
\end{aligned}\right\}$$

where k given in equation (21).

The displacement and stresses may be considered as constant function in elastic composites and operator functions of time in viscoelastic composites. The forms of stresses and displacement are now functions of (r,z,ω). In general, $u_\theta,\sigma_{r\theta},$ and $\sigma_{\theta z}$ can be represented according to Illyushin's approximation method (Allam et al, 1976 [12], 2005 [10], 2008 [13]) of the unified form:

$$f(r,z,\omega)=\sum_{i=1}^{5}A_i(r,z)\varphi_i(\omega), \tag{22}$$

where $f(r,\omega)$ is one of the functions $u_\theta,\sigma_{r\theta},$ and $\sigma_{\theta z}$

$$\left.\begin{aligned}
&\varphi_1=1,\quad \varphi_2=\omega,\quad \varphi_3=\pi=\frac{1}{\omega},\\
&\varphi_4=g_{1/2}(\omega),\quad \varphi_5=g_2(\omega)
\end{aligned}\right\} \tag{23}$$

where $g_\chi(\omega)=\frac{1}{1+\chi\omega}$, $\chi=\frac{1}{2},2$

The constants A_i , $(i=1,\ldots,5)$ are constants to be found from the system of linear algebraic equations.

$$L_{ij} A_j = B_i ,$$
$$L_{ij} = \int_0^1 \varphi_i(\omega)\, \varphi_j(\omega) d\omega, \tag{24}$$
$$B_i = \int_0^1 f(r, z, \omega) \varphi_i(\omega)\, d\omega, \qquad (i, j = 1, \ldots, 5)$$

Assuming an exponential relaxation function:

$$\omega = a_1 + b_1 e^{-\alpha t}, \tag{25}$$

where a_1, b_1, α are constants determined experimentally.

The Laplace-Carlson transformation is defined by,

$$F(p) = p \int_0^\infty e^{-px} f(x) dx ,$$

this transformation may be used to determine the functions $\pi(t)$ and $g_\chi(\omega), \quad \chi = \frac{1}{2}, 2$.

Denoting the transformations of $\pi(t), g_\beta(t)$ by $\pi^* = \frac{1}{\omega^*}, \quad g_\chi^* = \frac{1}{1+\chi\omega^*}$,

since $\omega^*(s) = a_1 + \frac{b_1 s}{(s+\alpha)}$, thus

$$\pi(t) = \frac{1}{a_1}\left\{1 - \frac{b_1}{a_1 + b_1} e^{\frac{-a_1\tau}{a_1+b_1}}\right\} \quad , \quad \tau = \alpha t ,$$
$$g_\chi(t) = \frac{1}{1+\chi a_1}\left[1 - \frac{\chi b_1}{1+\chi(a_1+b_1)} e^{\frac{-(1+\chi a_1)\tau}{[1+\chi(a_1+b_1)]}}\right], \quad \chi = \frac{1}{2}, 2. \tag{26}$$

The equation (22) for a viscoelastic composite may be recorded to obtain the explicit formulae for $f(r, z, \omega)$ as function of (r, z, t). Thus we have:

$$f(r, z, t) = A_1(r, z)\Omega(t) + A_2(r, z)\int_0^t \omega(t-\tau) d\Omega(\tau) +$$
$$A_3(r, z)\int_0^t \pi(t-\tau) d\,\Omega(\tau) + A_4(r, z)\int_0^t g_{\frac{1}{2}}(t-\tau) d\,\Omega(\tau) +$$
$$A_5(r, z)\int_0^t g_2(t-\tau) d\Omega(\tau),$$

Suppose that the twisted moment of the shaft increases linearly with time t and then becomes constant after time t_0, then the twisted angle Ω may written in the form

$$\Omega(t)=\begin{cases}\Omega_0 t & 0\le t\le t_0\\ \Omega_0 h(t-t_0) & t\ge t_0\end{cases} \tag{27}$$

where Ω_0 is constant, t_0 is the initial time of constant twisting moment rotation, and $h(t)$ is the Heaviside unit step function, then we have

$$f(r,z,t)=\sum_{j=1}^{5}A_j(r,z)X_j \tag{28}$$

where

$$X_1=\begin{cases}t & 0\le t\le t_0\\ h(t-t_0) & t\ge t_0\end{cases}$$

$$X_2=\begin{cases}-F_1(1)+2a_1t_0 & 0\le\tau\le t_0\\ a_1+F_2(1) & \tau\ge t_0\end{cases},$$

$$X_3=\begin{cases}\dfrac{1}{a_1^{\,2}}F_1\left(\dfrac{a_1}{a_1+b_1}\right) & 0\le\tau\le t_0\\ \dfrac{1}{a_1}\left(1-\dfrac{F_2\left(\dfrac{a_1}{a_1+b_1}\right)}{(a_1+b_1)}\right) & \tau\ge t_0\end{cases},$$

$$X_4=\begin{cases}\dfrac{2}{(2+a_1)^2}\left(F_1\left(\dfrac{2+a_1}{2+a_1+b_1}\right)-2t_0\right) & 0\le\tau\le t_0\\ \dfrac{2}{(2+a_1)}\left(1-\dfrac{F_2\left(\dfrac{2+a_1}{2+a_1+b_1}\right)}{(2+a_1+b_1)}\right) & \tau\ge t_0\end{cases},$$

$$X_5 = \begin{cases} \dfrac{1}{(1+2a_1)^2}\left(2F_1\left(\dfrac{1+2a_1}{1+2a_1+2b_1}\right)-t_0\right) & 0 \le \tau \le t_0 \\ \dfrac{1}{(1+2a_1)}\left(1-\dfrac{2F_2\left(\dfrac{1+2a_1}{1+2a_1+2b_1}\right)}{(1+2a_1+2b_1)}\right) & \tau \ge t_0 \end{cases},$$

Here $F_1(y) = b_1 e^{-y\tau} + a_1 t_0 - b_1 e^{-y(\tau - t_0)}, \quad F_2(y) = b_1 e^{-y(\tau - t_0)}$

4 Numerical Example and Discussion

A numerical example for torsion of anisotropic reinforced viscoelastic layer will be given. the example includes the layer of elastic and viscoelastic form. Computations were carried out for the following values of dimensionless parameters:

$$\frac{a}{h} = \frac{2}{3}, \quad \upsilon = \frac{1}{3}, \quad \xi = \frac{4}{3}, \quad \gamma = \frac{1}{10},$$
$$\Omega_0 = 5, \quad t_0 = 10, \quad a_1 = 0.1, \quad b_1 = 0.9,$$

The coefficient α depends on the scale of time parameter and let $\tau\ (\equiv \alpha t)$

The numerical examples of the stresses and displacement are calculated by using the following data:

Table 1

material	**value of** $k = \frac{G_{23}}{G_{12}}$
Anisotropic	0.5
Isotropic	1
Anisotropic	2

The results of the present investigations are given in Tables (2-8). Note that the results are given for different values of the geometrical and constitutive parameters.

Figs. (2)-(6) show the stresses and displacement in the dimensionless form:

$$\bar{u} = \frac{u}{\Omega_0}, \quad \bar{\sigma}_{\theta z} = \frac{\sigma_{\theta z}}{\Omega_0 G_{23}}, \quad \bar{\sigma}_{r\theta} = \frac{\sigma_{r\theta}}{\Omega_0 G_{12}},$$

and then we will remove the bars symbol.

The variations of the displacement u outside the shaft $(z=0)$ with r for all cases of constitutive parameter k are illustrated in Fig. (2), from which we see that the displacement u is rapidly decreased away from the shaft.

The distribution of the stress component $\sigma_{\theta z}$, on the contact surface under shaft $(z=0, 0\le r\le a)$ is plotted in Fig. (3), and at the fixed base $(z=h)$ in Fig. (4), we see that the component of stress $\sigma_{\theta z}$ under the shaft increases to attained its maximum value at the boundary of the shaft $\left(\bar{r}=\frac{r}{a}=1\right)$, while at the fixed base $\sigma_{\theta z}$ decreases far from the axis of the shaft. Also, the stress component $\sigma_{r\theta}$ on the contact surface $(z=0)$ is plotted in Fig. (5) , which shows that it increases under the shaft and decreases far from the shaft, the maximum value is attained at the shaft's boundary.

Fig. (6) shows the variations of stresses $\sigma_{\theta z}, \sigma_{r\theta}$ and displacement u at the middle plane of the layer with r, from which we noticed the discontinuity of $\sigma_{r\theta}$ at $(r=1)$ and all $|\sigma_{\theta z}|, |\sigma_{\theta r}|, |u|$ are rapidly decrease (absolutely) for $(r\ge 1)$ to vanished at biggest enough r. The stress component $\sigma_{\theta z}$ on the fixed base surface increases with r and attained its maximum at the boundary of the circle $(r=1)$, also in Fig. (6), the stress components $\sigma_{\theta z}, \sigma_{r\theta}$ has the same behavior of the displacement. The influence of ratio $\frac{a}{b}$, (radius of shaft /thickness of layer), on the distribution and magnitude is relatively insignificant.

Figs. (7) and (8) represent the vertical distribution at some points inside and outside of the area under the shaft $(r=0.2,\ r=2)$ of the stresses and displacement, from which we show that the values of stresses and displacement at points under the shaft at all levels z is too large compared with that outside the shaft at all levels z

Figs. (9)-(12) show the type of relaxation with time that occurs in the $u_\theta, \sigma_{r\theta}, \sigma_{\theta z}$ respectively at some particular points of the disk at $(r=0.3,\ r=3)$ for the top and bottom bases $z=0,\ z=h$, from which we see that all values are start to decrease (or increase) with time, and then increase (or decrease) to attained their asymptotic values, meaning that a steady state established in the layer.

Tables (2-8) give the values of coefficient A_i , $i=1,2,3,4,5$ given in equation (28) for the $u_\theta, \sigma_{r\theta}, \sigma_{\theta z}$ in terms of radius r at different levels z , from which we can deduce the viscoelastic solution at different values of r as explicit functions of the time.

5 Conclusion

A refined analytical solution to the problem of torsion of anisotropic layer is constructed, in this solution, some terms which canceled by Tang, 1979 are added, and the full solution is given in terms of r,z . The corresponding principal and Illyushin's approximation method are used to deduce the solution for the structurally anisotropic viscoelastic layer the solution is given numerically as explicit values of time.

The numerical example shows the behavior of the displacement and stresses in both cases elastic and viscoelastic composite layers with the variations of coordinates or time, and shows that a steady state will established in the layer.

6 Open Problems

In recent years, composite materials have gained considerable attention in many engineering applications. The composite structure is commonly defined as a combination of two or more distinct materials, each of which retains its own distinctive properties, to create a new material with properties that cannot be achieved by any of the components acting alone. Using this definition, it can be determined that a wide range of engineering materials fall into this category.
In this paper we consider the problem of a structurally anisotropic viscoelastic layer with fixed base when it is twisted by means of an attached rigid cylindrical shaft has many open problems which deserve to be treated. In this way we can mentioned the following:

1- The problem of structurally anisotropic viscoelastic layer when it is twisted by means of an attached two rigid cylindrical shafts on the upper and lower surfaces.

2- An infinite sandwich model containing three isotropic layers, the first and third one are made of elastic material, and the middle layer is made of viscoelastic material. A study is made on formal solution of the stresses and displacements, which occurred in this model, when it is twisted by means of turning a rigid cylindrical shaft attached to it.

3- An infinite layer made from functionally graded material when it is twisted by a cylindrical shaft at the upper surface.

References:

[1] C.J., Tranter, Integral Transform in Mathematical Physics, *John Wiley and Sons, Inc., New York* (1962).

[2] E.T., Whittaker, G.N., Watson, A Course of Modern Analysis, (4th Ed.), *Cambridge University Press* (1965).

[3] G.N., Watson, A Treatise on the Theory of Bessel Functions, (2nd Ed.), *Cambridge University Press* (1966).

[4] H., Dewa, Torsional Stress Analysis and Vibration Damping of Three Layered Rods, *JSME International Journal* 33 (2) (1989) 152–159.

[5] Ian N., Sneddon, Mixed Boundary Value Problems in Potential Theory, *North-Holland Publishing Co. Amsterdam* (1966).

[6] J.Q., Tarn, H.H., Chang, Torsion of Cylindrically Orthotropic Elastic Circular Bars with Radial Inhomogeneity Some Exact Solutions and End Effects, *International Journal of Solids and Structures* 45 (2008) 303-319.

[7] K.L., Napolitano, J.B., Kosmatka, Co-Cured Extension Twist Coupled Damped Composite Strut, *Journal of Composite Materials* 32 (21) (1998) 1914–1932.

[8] L.W., Chen, W., Kung Peng, The Stability Behavior of Rotating Composite Shafts Under Axial Compressive Loads, *Composite Structure* 41 (1998) 253–63.

[9] M.N.M., Allam, A.F., Ghaleb, Torsion of a Composite, Viscoelastic Prismatic Bar of Rectangular Cross-Section, *Applied Mathematical Modelling* 6 (1982) 197–201.

[10] M.N.M., Allam, A.M., Zenkour, On the Rotating Fiber Reinforced Viscoelastic Composite Solid and Annular Disks of Variable Thickness, *Int J. Comput. Methods Eng. Sci. Mech.* 7 (2005) 21-31.

[11] M.N.M., Allam, A.M., Zenkour, Bending Response of a Reinforced Viscoelastic Arched Bridge Model, *Applied Mathematical Modelling* 27 (2003) 233–248.

[12] M.N.M., Allam, B.E., Pobedria, On the Solution of Quasi-Statical Problems of Anisotropic Viscoelasticity, *Isvestia Akademy Nauk, AR-SSR Mekhanika* 31 (1976) 19–27 (in Russian).

[13] M.N.M., Allam, R.E., Badr, R., Tantawy, Stresses of a Rotating Circular Disk of Variable Thickness Carrying a Current and Bearing a Coaxial Viscoelastic Coating, *Applied Mathematical Modelling* 32 (2008) 1643–1656.

[14] M.M., Shokrieh, A., Hasani, L.B, Lessard, Shear Buckling of a Composite Drive Shaft Under Torsion, *Composite Structures* 64 (2004) 63–69.

[15] R.C., Tang, Torsion of Anisotropic Layer, *Applied Science Publishers Ltd, England* (1979).

[16] S.A., Aseeri, Goursat Functions for a Problem of an Isotropic Plate With a Curvilinear Hole , *international Journal of Open Problems in Computer Science and Mathematics* 1 (3) (2008) 266–285.

[17] S.A., Nayfeh, K.K., Varanasi, A Model for The Damping of Torsional Vibration in Thin Walled Tubes With Constrained Viscoelastic Layers, *Journal of Sound and Vibration* 278 (2004) 825–846.

[18] S.G., Lekhnitiskii, Anisotropic Plates, *Gordon and Breach Science Publishers, New York* (1968).

[19] T., Nouri-Baranger, P., Trompette, S., Shakhesi, Torsional Vibrations of Laminated Beams Comparison of Models, *Proceedings of the ASME Design Engineering Technical Conferences* Vol. 7B, Las Vegas, NV (1999) 3113–3120.

Appendix:

a)
$$\begin{cases} B(k)=\sum_{i=1}^{3}A_{i-1}\left(\sum_{q=0}^{\infty}(-1)^q\sum_{m=0}^{\infty}u_k(i,1)\ -\sum_{q=0}^{\infty}(-1)^q\sum_{m=0}^{\infty}u_k(i,2)\right), & \mathrm{k}=1,2,3 \\ B_1(k)=\sum_{i=1}^{3}H_{i-1}\left(\sum_{q=0}^{\infty}(-1)^q\sum_{m=0}^{\infty}u_k(i,1)\ -\sum_{q=0}^{\infty}(-1)^q\sum_{m=0}^{\infty}u_k(i,2)\right), & \mathrm{k}=4,5,6 \end{cases},$$

and

b)
$$\begin{cases} u_1(i,j)=\dfrac{u_0a^{2i}\Gamma(2i+1+2m)}{\left(a^2+v_j^{\,2}\right)^{\left(\frac{2i+1}{2}+m\right)}}\ {}_2F_1\left(\frac{2i-1}{2}-m,\frac{2i+1}{2}+m;\frac{4i+1}{2};\frac{a^2}{a^2+v_j^{\,2}}\right) \\ u_2(i,j)=\dfrac{u_0a^{2i}\Gamma(2i+2+2m)}{\left(a^2+v_j^{\,2}\right)^{(i+1+m)}}\ {}_2F_1\left(i-1-m,i+1+m;\frac{4i+1}{2};\frac{a^2}{a^2+v_j^{\,2}}\right) \\ u_3(i,j)=\dfrac{\left(\frac{r}{2}\right)u_2(i,j)}{(2+m)} \end{cases}$$

c)
$$\begin{cases} u_4(i,j)=\dfrac{(-1)^m}{m!}\dfrac{\left(\frac{a}{2}\right)^{(2i+2m)}\Gamma(2i+1+2m)}{\Gamma\left(\frac{2i+1}{2}+m\right)\left(r^2+v_j^{\,2}\right)^{\left(\frac{2i+1}{2}+m\right)}}\ {}_2F_1\left(i-1-m,\frac{2i+1}{2}+m;2;\frac{r^2}{r^2+v_j^{\,2}}\right) \\ u_5(i,j)=\dfrac{(-1)^m\left(\frac{a}{2}\right)^{(2i+2m)}\Gamma(2i+2+2m)}{m!\Gamma\left(\frac{4i+1}{2}+m\right)\left(r^2+v_j^{\,2}\right)^{(i+1+m)}}\ {}_2F_1\left(i+1+m,-\frac{2i-1}{2}-m;2;\frac{r^2}{r^2+v_j^{\,2}}\right) \\ u6(i,j)=\dfrac{(-1)^m\left(\frac{a}{2}\right)^{(2i+2m)}\Gamma(2i+3+2m)}{m!\Gamma\left(\frac{4i+1}{2}+m\right)\left(r^2+v_j^{\,2}\right)^{\left(\frac{2i+3}{2}+m\right)}}\ {}_2F_1\left(1-i-m,\frac{2i+3}{2}+m;3;\frac{r^2}{r^2+v_j^{\,2}}\right) \end{cases}$$

where ${}_2F_1(\upsilon,\mu;\gamma;\lambda)$ is the hypergeometric function,

$$A_0=\frac{H_0}{3},\quad A_1=\frac{H_1}{35},\ \textit{and}\quad A_2=\frac{H_2}{5465}$$

$$v_1=2qb+\frac{z}{\sqrt{k}},\qquad v_2=2qb+2b-\frac{z}{\sqrt{k}}$$

$$u_0=\frac{(-1)^m\left(\frac{r}{2}\right)^{(1+2m)}}{m!\Gamma(2+m)},\quad i=1,2,3\ \textit{and}\ j=1,2$$

d) For $\underline{0<b<a}$

$$\int_0^{\infty} \frac{J_{\alpha-\beta}(at)J_{\gamma-1}(bt)}{t^{\gamma-\alpha-\beta}}dt = \sum_{m=0}^{\infty} \frac{(-1)^m b^{\gamma+2m-1}\Gamma(2\alpha+2m)\Gamma\left(\frac{1}{2}\right)}{m!\Gamma(\gamma+m)2^{\alpha-\beta+\gamma+2m-1}a^{\alpha+\beta+2m}\Gamma(1-\beta-m)\Gamma\left(\alpha+m+\frac{1}{2}\right)}$$

e) For $\underline{|z| < \sqrt{a^2+c^2}}$

$$\int_0^{\infty} e^{-ct} \frac{J_{\alpha-\beta}(at)J_{\gamma-1}(zt)}{t^{\gamma-\alpha-\beta}}dt = \sum_{m=0}^{\infty} \frac{(-1)^m\left(\frac{z}{2}\right)^{\gamma+2m-1}\left(\frac{a}{2}\right)^{\alpha-\beta}\Gamma(2\alpha+2m)}{m!\Gamma(\gamma+m)\left(a^2+c^2\right)^{\alpha+m}\Gamma(\alpha-\beta+1)} {}_2F_1\left(\alpha+m, \frac{1}{2}-\beta-m; \alpha-\beta+1; \frac{a^2}{a^2+c^2}\right)$$

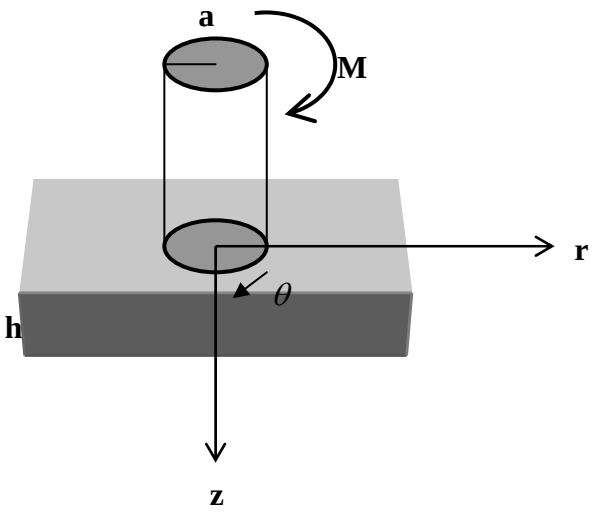

Fig. 1. Infinite anisotropic layer.

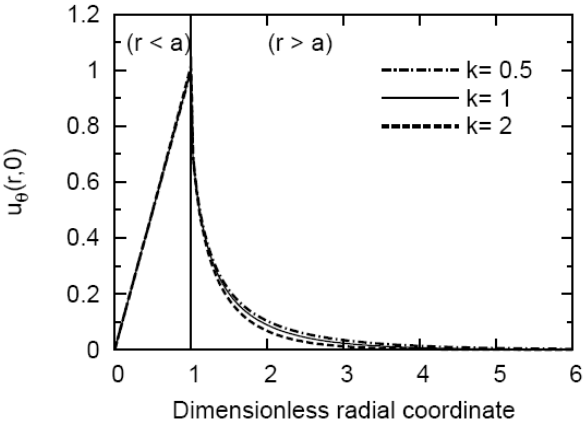

Fig. 2. Distribution of $u_\theta(r,0)$ with r.

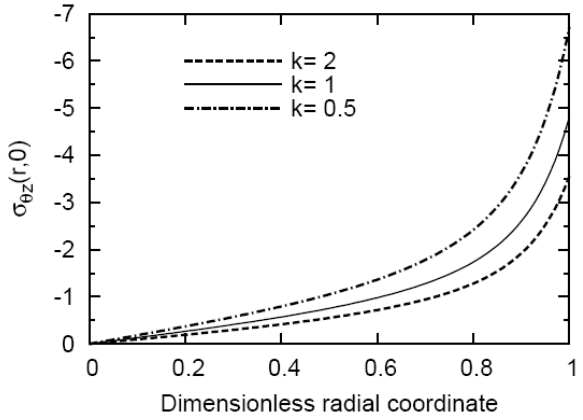

Fig. 3. Distribution of $\sigma_{\theta z}(r,0)$ for $0 \le r \le a$.

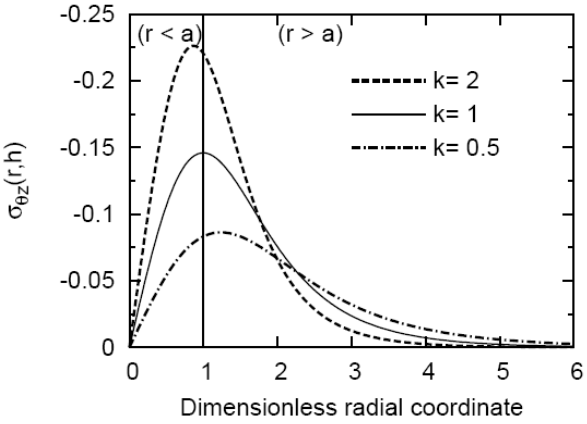

Fig. 4. Distribution of $\sigma_{\theta z}(r,h)$ with r.

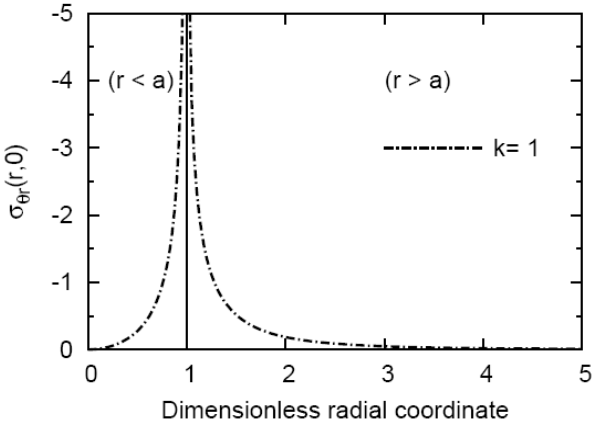

Fig. 5. Distribution of $\sigma_{\theta r}(r,0)$ with r.

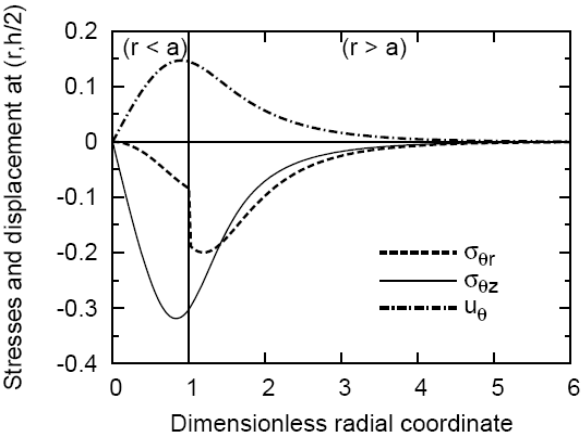

Fig. 6. Stresses and displacement at $z = \frac{h}{2}, k = 1$.

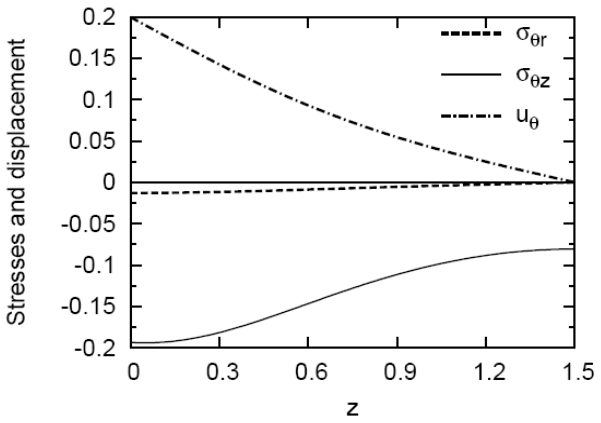

Fig. 7 . Stresses and displacement at $r = 0.2$, $k = 2$.

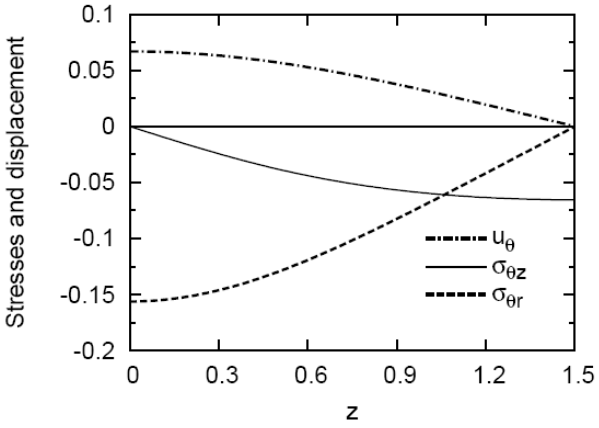

Fig. 8. Stresses and displacement at $r = 2$, $k = 2$.

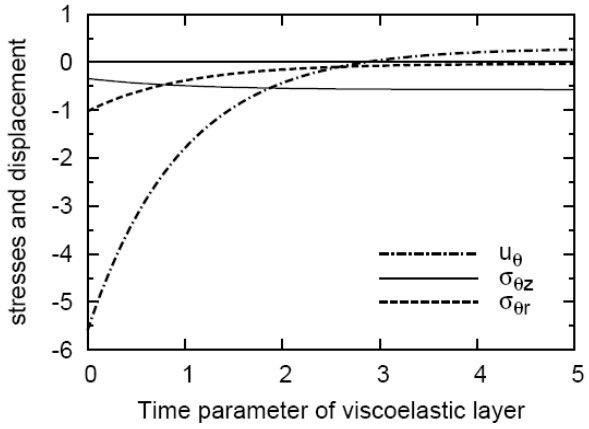

Fig. 9. Variation of stress and displacement at $(r = 0.3, z = 0)$ with time.

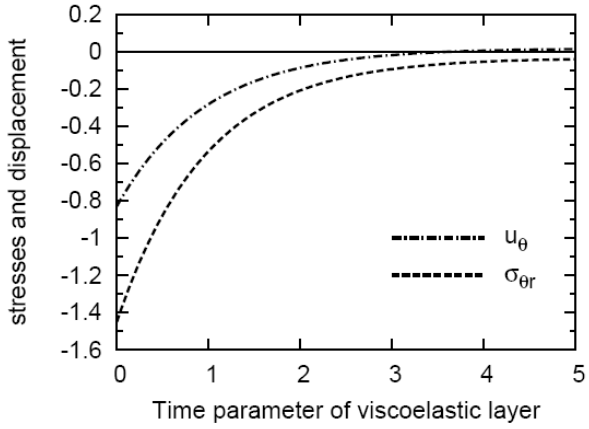

Fig. 10. Variation of stress and displacement at $(r = 3, z = 0)$ with time.

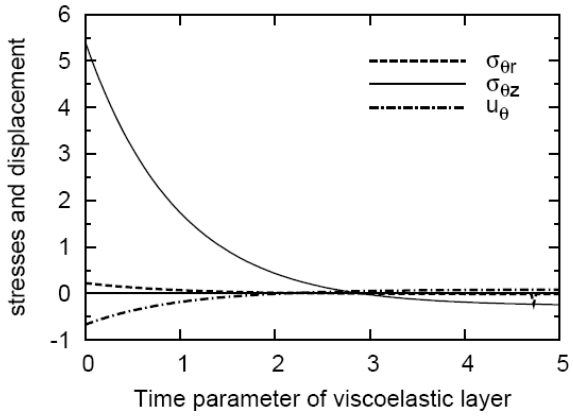

Fig. 11. Variation of stress and displacement at $(r = 0.3, z = \frac{h}{2})$ with time.

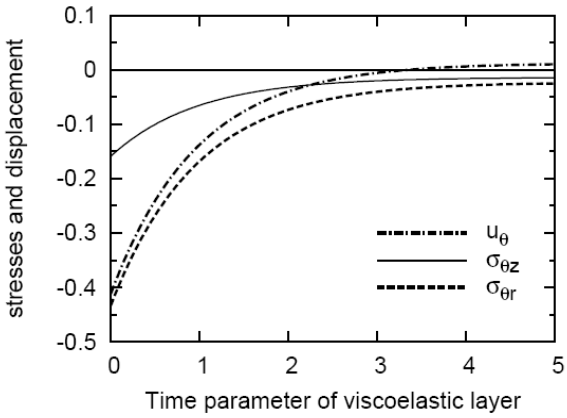

Fig. 12. Variation of stress and displacement at $(r = 3, z = \frac{h}{2})$ with time.

r	A_1 x10^{-2}	A_2 x10^{-7}	A_3 x10^{-8}	A_4 x10^{-6}	A_5 x10^{-7}
0	0	0	0	0	0
0.1	9.98861	135.807	1.68855	68.2639	-154.183
0.2	19.9846	177.115	2.09827	88.5736	-198.275
0.3	30.0225	-666.693	-8.35805	-335.394	758.657
0.4	40.0044	149.628	1.87337	75.2269	-170.022
0.5	50.0981	-1574.83	-19.6909	-792.123	1791.11
0.6	60.0224	1276.56	15.9867	642.127	-1452.19
0.7	70.1682	-1197.64	-15.0398	-602.620	1363.58
0.8	80.1529	588.536	7.4085	296.193	-670.462
0.9	90.2062	716.737	8.8396	359.904	-811.506
1	100.218	1782.74	21.9979	895.363	-2019.44
	78.5394	-1210.08	-14.7947	-607.089	1366.73
2	8.05911	-3.15764	-0.03819	-1.57502	3.51924
3	1.85255	-95.9726	-1.17423	-48.1527	108.419
4	0.47191	18.5754	0.23012	9.33259	-21.0625
5	0.12664	4.65379	0.05754	2.33768	-5.27404
6	0.03563	0.58522	0.00723	0.29392	-0.66292
7	0.01102	0.12797	0.00158	0.06428	-0.14502
8	0.00431	0.08776	0.00107	0.04402	-0.09908
9	0.00252	-0.10781	-0.00133	-0.05415	0.12216
10	0.00207	0.03652	0	0.01838	-0.04161

Table (2) Values of A_i for $u(r,0)$.

r	A_1	A_2 x10^{-4}	A_3 x10^{-7}	A_4 x10^{-3}	A_5 x10^{-4}
0	0	0	0	0	0
0.1	-0.18282	-0.39777	-0.49173	-0.19981	0.45079
0.2	-0.37114	-1.28973	-1.58763	-0.64756	1.45979
0.3	-0.57262	0.02612	0.01842	0.02431	-0.02541
0.4	-0.79487	0.48497	0.61916	0.24446	-0.5549
0.5	-1.05214	2.42826	3.00983	1.22012	-2.75407
0.6	-1.36315	-5.08364	-6.31142	-2.55488	5.76889
0.7	-1.78505	5.07556	0.06379	2.55443	-5.78183
0.8	-2.42082	5.47219	6.67828	2.74492	-6.17784
0.9	-3.62884	15.1039	18.5393	7.58186	-17.0844
1	-6.71095	16.2087	19.9344	8.13715	-18.3397

Table (3) Values of A_i for $\sigma_{\theta z}(r,0)$.

r	A_1	A_2 x10^{-5}	A_3 x10^{-7}	A_4 x10^{-5}	A_5 x10^{-5}
0	0	0	0	0	0
0.1	0.02987	1.16902	0.14541	5.87594	-1.32716
0.2	0.05897	1.02107	0.12994	5.14531	-1.16721
0.3	0.08648	-0.85826	-0.10442	-4.30327	0.96784
0.4	0.11131	1.23207	0.15093	6.18272	-1.39248
0.5	0.13298	-3.10466	-0.38174	-15.5863	3.51289
0.6	0.14977	7.60472	0.93883	38.1941	-8.61468
0.7	0.16218	1.44551	0.18431	7.28641	-1.65372
0.8	0.16849	7.85152	0.98488	39.5049	-8.93791
0.9	0.16937	8.41702	1.04244	42.2896	-9.54444
1	0.16526	5.25937	0.64145	26.3782	-5.93547
	0.16544	-2.91445	-0.36888	-14.6786	3.32672
2	0.05302	-2.00364	-0.24906	-10.0707	2.27439
3	0.013	-0.47976	-0.05929	-2.40998	0.54371
4	0.3341	-0.07301	-0.00907	-0.36692	0.08285
5	0.00089	-0.0099	-0.00126	-0.04988	0.01131
6	0.00025	-0.00715	-0.0009	-0.03603	0.00816
7	0.00007	0.00144	0.00018	0.00724	-0.00163
8	0.00002	-0.00184	-0.00023	-0.00924	0.00208
9	0.00001	0.00029	0.00003	0.00147	-0.00033
10	0.00001	0.00003	0	0.00019	-0.00004

Table (4) Values of A_i for $\sigma_{r\theta}(r,0)$.

r	A_1	A_2 x10^{-5}	A_3 x10^{-7}	A_4 x10^{-5}	A_5 x10^{-5}
0	0	0	0	0	0
0.1	0.02995	1.01988	0.12594	5.1223	-1.15536
0.2	0.05924	-1.86723	-0.23169	-9.38314	2.11839
0.3	0.08657	2.64318	0.32838	13.2846	-3.00001
0.4	0.11169	-1.07658	-0.13271	-5.40639	1.21914
0.5	0.13327	-1.65163	-0.20526	-8.3019	1.87506
0.6	0.15052	-1.63526	-0.19709	-8.19146	1.83918
0.7	0.16268	-0.93821	-0.12049	-4.73308	1.0757
0.8	0.16933	-2.40829	-0.30332	-12.1227	2.74484
0.9	0.16973	10.2984	1.2737	51.7337	-11.6727
1	0.16603	-3.61649	-0.44937	-18.1764	4.10472
	0.16571	0.77139	0.090859	3.85488	-0.86186
2	0.05316	-2.14744	-0.26856	-10.8013	2.44241
3	0.01304	-0.49858	-0.06137	-2.50323	0.56428
4	0.00335	-0.19103	-0.02375	-0.96021	0.21688
5	0.00089	-0.00377	-0.00045	-0.01889	0.00424
6	0.00025	0.01213	0.00149	0.06091	-0.01373
7	0.00008	-0.00059	-0.00007	-0.00297	0.00067
8	0.00003	-0.00157	-0.00019	-0.00789	0.00178
9	0.00001	0.00046	0.00006	0.00229	-0.00052
10	0.00001	-0.00021	-0.00003	-0.00108	0.00024

Table (5) Values of A_i for $u\left(r,\frac{h}{2}\right)$.

r	A_1	A_2 x10^{-5}	A_3 x10^{-7}	A_4 x10^{-5}	A_5 x10^{-5}
0	0	0	0	0	0
0.1	-0.09467	0.46214	0.05439	2.30848	-0.51588
0.2	-0.18753	-0.94139	-0.11164	-4.70732	1.05369
0.3	-0.277	6.43789	0.80469	32.3774	-7.31983
0.4	-0.36003	9.29524	1.15049	46.6951	-10.5364
0.5	-0.43248	-13.1587	-1.58281	-65.9024	14.7918
0.6	-0.49305	11.0627	1.39095	55.671	-12.5997
0.7	-0.53346	-8.72125	-1.11029	-43.9501	9.97093
0.8	-0.55303	20.1745	2.50159	101.374	-22.8845
0.9	-0.54538	-7.94924	-1.00098	-40.0144	9.06016
1	-0.51794	18.9767	2.37293	95.4451	-21.5805
	-0.32488	-12.1098	-1.51208	-60.8934	13.7632
2	-0.06315	1.43524	0.17523	7.19988	-1.62059
3	-0.01377	-0.16382	-0.01964	-0.82009	0.18393
4	-0.00349	-0.0582	-0.00716	-0.29223	0.06587
5	-0.00094	-0.00633	-0.00076	-0.03173	0.00712
6	-0.00026	-0.00368	-0.00048	-0.01858	0.00424
7	-0.00008	0.00148	0.00018	0.00742	-0.00167
8	-0.00003	0.00188	0.00023	0.00942	-0.00212
9	-0.00001	-0.00139	-0.00017	-0.007	0.00158
10	-0.00001	0.00005	0	0.00259	-0.00058

Table (6) Values of A_i for $\sigma_{\theta z}\left(r,\frac{h}{2}\right)$.

r	A_1	A_2 x10^{-5}	A_3 x10^{-8}	A_4 x10^{-5}	A_5 x10^{-5}
0	0	0	0	0	0
0.1	-0.00321	-0.11006	-0.13238	-0.55121	0.12372
0.2	-0.01301	0.28271	0.34564	1.41844	-0.31936
0.3	-0.02975	-1.12524	-1.42785	-5.66782	1.28487
0.4	-0.05438	-1.32583	-1.64084	-6.66065	1.50301
0.5	-0.08837	2.24001	2.77395	11.254	-2.53982
0.6	-0.13357	-3.48599	-4.33879	-17.5238	3.95857
0.7	-0.19444	-11.2653	-13.9254	-56.5859	12.7657
0.8	-0.28073	8.80212	10.8977	44.2224	-9.98002
0.9	-0.41227	21.4652	27.0274	108.039	-24.4591
1	-0.65563	20.8445	25.5752	104.626	-23.5728
	-4.85197	-161.493	-196.988	-810.036	182.293
2	-0.16903	10.6223	13.2077	53.3922	-12.0592
3	-0.03196	-1.60321	-1.97569	-8.05065	1.81527
4	-0.0075	0.13288	0.16374	0.66729	-0.15047
5	-0.00189	0.04735	0.05858	0.23786	-0.05368
6	-0.0005	0.00522	0.00652	0.02626	-0.00593
7	-0.00014	-0.0041	-0.00511	-0.02065	0.00467
8	-0.00004	0.00013	0	0.00065	-0.00015
9	-0.00001	0.00024	0	0.00122	-0.00028
10	0	0	0	-0.00027	0.00005

Table (8) Values of A_i for $\sigma_{\theta z}\left(r,h\right)$.

r	A_1	A_2 x10^{-5}	A_3 x10^{-7}	A_4 x10^{-5}	A_5 x10^{-5}
0	0	0	0	0	0
0.1	-0.00145	-0.04879	-0.00609	-0.24535	0.05544
0.2	-0.00578	-0.06261	-0.00774	-0.31449	0.07096
0.3	-0.01289	0.26841	0.03302	1.34755	-0.30373
0.4	-0.02257	0.72969	0.09116	3.66962	-0.82954
0.5	-0.03436	-1.60832	-0.19827	-8.07633	1.82110
0.6	-0.04799	-0.55553	-0.06843	-2.78921	0.62878
0.7	-0.06247	-2.65839	-0.32884	-13.3542	3.01311
0.8	-0.07707	-1.68291	-0.20627	-8.44581	1.90242
0.9	-9.05834	0.05391	0.00694	0.27215	-0.06191
1	-0.10185	-0.63268	-0.0761	-3.16805	0.71089
	-0.23515	15.8958	1.97376	79.8871	-18.0387
2	-0.10105	-1.96796	-0.24176	-9.87844	2.22597
3	-0.02227	-0.464	-0.05595	-2.32467	0.52207
4	-0.00529	-0.14615	-0.01791	-0.73345	0.16521
5	-0.00134	-0.03657	-0.00449	-0.18359	0.04137
6	-0.00035	-0.01337	-0.00166	-0.06722	0.01518
7	-0.00009	-0.00119	-0.00015	-0.00604	0.00137
8	-0.00002	0.00078	0.00009	0.00392	-0.00088
9	0	-0.00012	-0.00001	-0.00059	0.00013
10	0	0.00012	0.00001	0.00062	-0.00014

Table (7) Values of A_i for $\sigma_{r\theta}\left(r,\frac{h}{2}\right)$.